IEEE Robotics and Automation Letters (RA-L) paper, presented at ICRA 2023, London, UK. Cite as RA-L paper.

Adaptive Cooperative Control for Human-Robot Load Manipulation

Carlos R. de Cos[1,2] and Dimos V. Dimarogonas[1]

***Abstract*—In this letter, we propose a control strategy for human-robot cooperative manipulation under the *ambiguous* collaboration of a human agent. To cope with this uncertainty, an adaptive update law inferring the human contribution to the system dynamics from basic perception feedback through the human arm stiffness is used. Furthermore, the robustness and accuracy of the approach is enhanced by redundantly tracking the shared load references and its associated end-effector position references. To validate the control strategy, both theoretical Lyapunov stability analysis and experimental results –employing two robot manipulators with 6 degrees of freedom under external disturbances– are provided.**

***Index Terms*—Human-robot collaboration, robust/adaptive control, multi-robot systems.**

I. Introduction

In the last decades, robot manipulation has reached the technological maturity required to perform repetitive complex tasks autonomously. Increasingly accurate and reliable controllers have been implemented, with a substantial impact on the industry. However, these have been mainly designed for single robot applications or predictable multi-robot routines thus rendering fluent interaction capabilities with unstructured environments still challenging today [1]. This has hindered interaction-based applications in which the use of human operators is currently unavoidable. In this context, the paradigm of human-robot collaboration [2] has emerged as a trade-off solution combining the hard-to-replicate human experience and the enhanced capabilities of robot manipulators. In particular, human-robot collaboration is expected to play an essential role in agricultural robotics [3], an important –but yet vastly human-powered– sector. The implementation of such paradigm, nonetheless, demands the design of flexible and robust controllers that specifically consider those interaction capabilities in their formulation.

We discuss here the base of current approaches fulfilling this demand and their inherent drawbacks. Safe passive controllers [4], variable/adaptive impedance controllers for human-robot interaction [5]–[8] and classic impedance solutions without update using haptic feedback [9], [10] ensure a robust response, but generally lack the accuracy required for agricultural robotics, do not explicitly consider the interaction in the formulation, or depend excessively on the operator input. In contrast, solutions estimating the human's desired motion to reduce human effort for human-provided trajectories [11] or to shape these trajectories [12] are capable of providing enhanced collaboration capabilities, but are again highly dependent on the human input, and either demand considerable computational load due to their implicit formulation [12], or lack the accuracy for the proposed application due to the use of an impedance controller for the inner control loop [11]. Other alternatives include learning from demonstration to adjust the operational space stiffness [13], but requiring slow human demonstration to change the design task; employing projected inverse dynamics control to compensate induced dynamics and provide and impedance behaviour [14], with the aforementioned limitations of such response; using single-agent adaptive sliding mode control to guarantee the fulfilment of the task (i.e. attitude) while the operator guides the load via direct force feedback [15], hence requiring force sensing capabilities; and solutions to detect and classify interactions to act according to predefined responses as a first step towards unstructured human-robot interaction [16], [17].

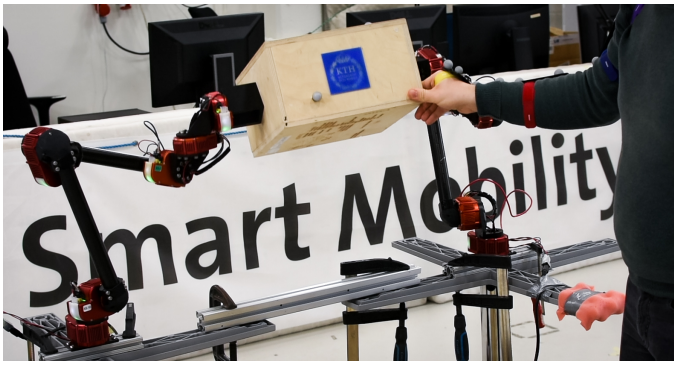

Fig. 1. Experimental validation of the control strategy. These were carried out by C. R. de Cos, the first author, at the SML facilities in KTH [18].

Moreover, it is worth mentioning potentially interesting alternatives that are not specifically designed for human-robot interaction. In [19] an adaptive control strategy in SE(3) is used to track both load position and attitude but it requires continuous excitation to reach its full potential; [20] employs an adaptive inverse kinematics solution for band-limited communications, but possible human interaction is limited to pre-defining desired motions; and in [21] adaptive contact stiffness is used to provide force control capabilities against uncharacterised surfaces for single agents.

Manuscript received: November, 11, 2021; Revised January, 10, 2022; Accepted February, 28, 2022.

This paper was recommended for publication by Editor Angelika Peer upon evaluation of the Associate Editor and Reviewers' comments. This work was supported by the Swedish Research Council (VR), the Swedish Foundation for Strategic Research (SSF), the Knut and Alice Wallenberg Foundation (KAW), the H2020 CANOPIES project, and the ERC LEAFHOUND project.

[1]Division of Decision and Control Systems, KTH Royal Institute of Technology, Stockholm, 114 28, Sweden.

[2]MathWorks AB, Kista, 164 40, Sweden. Email: cdecos@mathworks.com.

Digital Object Identifier (DOI): see top of this page.

IEEE Robotics and Automation Letters (RA-L) paper, presented at ICRA 2023, London, UK. Cite as RA-L paper.

Specifically, in the CANOPIES project [22] we require control strategies capable of dealing with the unpredictability of human behaviours, such as [23] and [24], but for a team of heterogeneous robots collaborating with human operators to harvest and prune table grapes. For this reason, we propose an approach characterised by the following contributions:

C1. The *ambiguous* –i.e. not inherently positive or negative– human contributions are indirectly inferred from basic perception feedback and fed via an adaptive update law to mitigate negative external disturbances without undermining possible positive contributions.

C2. To the best of the authors' knowledge, this is the first controller for human-robot collaboration tracking both i) the reference of the load shared between the manipulators and the human, ii) and its derived end-effector references; at the same time and consistently.

The impact of C2 on the robustness of the solution is twofold. Firstly, the subtask associated with the end-effectors reduces the impact of uncertainties of the load model and incorporates the complex nature of manipulators. And secondly, the subtask for the load itself handles the interaction between the different manipulators efficiently. To validate these contributions, the stability of the strategy is analysed using Lyapunov functions; and the controller is implemented on a system comprised of two robot manipulators, a human agent –that, depending on the scenario, contributes to the task or disturbs it–, and a shared load (see Fig. 1).

The rest of the letter is structured as follows: Section II specifies the model of the system controlled with the strategy proposed in Section III, while Section IV is focused on analysing the experimental results to validate the approach. Finally, the letter includes a conclusions Section V.

A. Notation

All vectors are column vectors and their references are identified with the subindex r. By default, these are expressed in the inertial reference frame $\{\mathcal{I}\}$ with origin O, but they can also be written in the load body frame $\{\mathcal{B}\}$, with origin in its CoG (see Fig. 2). Sub-indexes in capital letters refer to agents (in parenthesis in the text), i.e. π_A identifies the variable π associated with agent (A). $I_S, 0_S$ denote –respectively– the identity and zero matrices of size S and $\mathbf{0}_S$ the zero column vector of length S; J denotes the geometric Jacobian of an RM as in [25]; $M^\dagger, M^+$ the left and right-hand Moore-Penrose pseudoinverses of matrix M, respectively; $\mathbf{v}^\times$ the cross product matrix for vector $\mathbf{v}$; and tr stands for the trace. The estimate of any variable π is denoted as $\hat{\pi}$, and its estimation error as $\tilde{\pi} := \pi - \hat{\pi}$. The concatenation of matrices can be succinctly shown in the text using the comma and semicolon notation, i.e.

$$(A, B; C, D) := \begin{pmatrix} A & B \\ C & D \end{pmatrix}.$$

Acronyms: robot manipulator (RM), end-effector (EE), roll pitch yaw (RPY), degree of freedom (DoF), centre of gravity (CoG), human-robot interaction (HRI), human-robot collaboration (HRC).

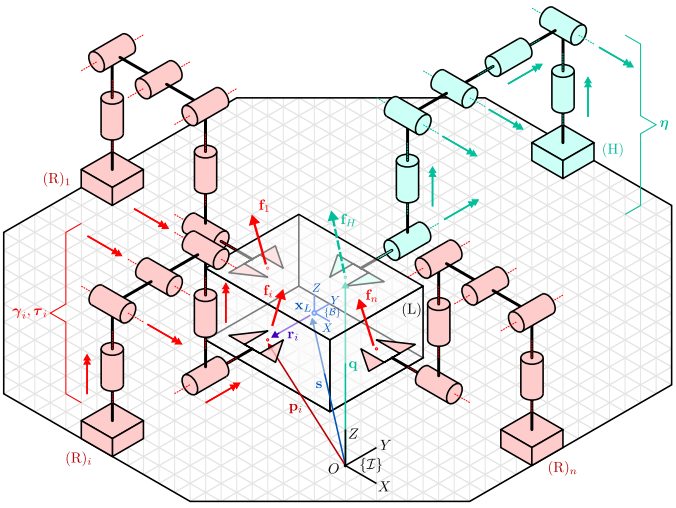

Fig. 2. Scheme of the system including the grasping setting –with (R) in red and (H) in aquamarine–, and $\{\mathcal{B}\}$ and $\{\mathcal{I}\}$ reference frames.

B. System and design task

Let us consider the system depicted in Fig. 2, composed by: a team of $n \geq 2$ robots (R) –each one equipped with a N_i-DoF RM, $N_i \geq 3$, $i = 1, ..., n$–; a human operator arm (H) –assumed equivalent to a 7-DoF RM, as in [25], [26] but enriched with flexible modes[1]–; and a rigid body (L) –whose load is shared by (R) and (H)–. Each of these agents is characterised by:

(R) joint-space configuration $\boldsymbol{\gamma}^\top := [\boldsymbol{\gamma}_1^\top, \cdots, \boldsymbol{\gamma}_n^\top] \in \mathbb{R}^N$, with $\boldsymbol{\gamma}_i \in \mathbb{R}^{N_i}$ the joint-space of the i^{th} agent and $N = \sum_{i=1}^n N_i$ the total number of DoF; and Cartesian EE positions $\mathbf{p}^\top := [\mathbf{p}_1^\top, \cdots, \mathbf{p}_n^\top] \in \mathbb{R}^{3n}$.

(H) joint-space configuration, including the angle of the links $\boldsymbol{\eta} \in \mathbb{R}^7$ and of the motors $\boldsymbol{\mu} \in \mathbb{R}^7$, where $\boldsymbol{\delta} := \boldsymbol{\eta} - \boldsymbol{\mu}$ are the flexible deflections (also denoted as flexible modes); and Cartesian EE position $\mathbf{q} \in \mathbb{R}^3$.

(L) CoG position $\mathbf{s} \in \mathbb{R}^3$ and attitude with respect to the base frame $\boldsymbol{\theta} := [\phi, \theta, \psi]^\top \in \mathbb{R}^3$ in RPY, and the fixed grasping points of both (R) and (H), namely $\mathbf{p}, \mathbf{q}$.

The design task for this system is to *simultaneously* track: i) the CoG position and attitude references of (L), $\mathbf{s}_r$ and $\boldsymbol{\theta}_r$, and ii) the EE position references of (R), $\mathbf{p}_r$; with the *ambiguous* (i.e. not *a priori* positive to the performance of the whole system) collaboration of (H). Accordingly, the task-space for each agent is defined as: $\mathbf{x}_L^\top := [\mathbf{s}^\top, \boldsymbol{\theta}^\top]$ for (L), $\mathbf{p}$ for (R), and $\mathbf{q}$ for (H); where the latter is not controllable, as (H) is an external ambiguous agent.

II. System Modelling

Considering the complex nature of the system, it is essential to specify the model used to design the controller. For that purpose, the kinematics and dynamics of the system are firstly presented. In addition, to design an update law coping with (H) uncertainties, a model of the dynamic interaction between (H) and (L) is proposed.

[1]Flexible modes describe the additional dynamic complexity induced by the extra flexible DoF, generally in the form of vibrations/oscillations.

A. Kinematics

Firstly, the kinematics of the task-space of the system is

$$\dot{\mathbf{x}}_L := \mathbb{T}_L^{-1}\mathbf{v}_L, \tag{1a}$$
$$\mathbf{v}_R := J_R\dot{\boldsymbol{\gamma}}, \tag{1b}$$
$$\mathbf{v}_H := J_H\dot{\boldsymbol{\eta}}, \tag{1c}$$

where $\mathbf{v}_R^\top := [\dot{\mathbf{p}}^\top, \boldsymbol{\omega}_R^\top]$ is the (R) operational-space velocity, with $\boldsymbol{\omega}_R$ the (R) angular velocity, and J_R is the geometric Jacobian of (R); J_H is the geometric Jacobian of (H), $\mathbf{v}_H^\top := [\dot{\mathbf{q}}^\top, \boldsymbol{\omega}_H^\top]$ is the (H) operational-space velocity, with $\boldsymbol{\omega}_H$ the (H) angular velocity; and $\mathbf{v}_L^\top := [\dot{\mathbf{s}}^\top, \boldsymbol{\omega}_L^\top]$ the corresponding one for (L), with $\boldsymbol{\omega}_L := T_L\dot{\boldsymbol{\theta}}$ the (L) angular velocity, and

$$T_L := \begin{pmatrix} \cos\psi\cos\theta & -\sin\psi & 0 \\ \sin\psi\cos\theta & \cos\psi & 0 \\ -\sin\theta & 0 & 1 \end{pmatrix}, \quad \mathbb{T}_L := \begin{pmatrix} I_3 & 0_3 \\ 0_3 & T_L \end{pmatrix}.$$

As the task only includes (R) and (H) Cartesian positions, let us also define their position Jacobians for simplicity –i.e. only using their associated rows in J_R, J_H–, namely

$$\dot{\mathbf{p}} := J_R^p\dot{\boldsymbol{\gamma}}, \quad \dot{\mathbf{q}} := J_H^p\dot{\boldsymbol{\eta}}.$$

B. Dynamics

On the one hand, using the Euler-Lagrange and Newton-Euler formalisms to respectively obtain the dynamic equations of (R) and (L) results in

$$M\dot{\mathbf{v}}_L + \boldsymbol{\omega}_L^\times I_L\boldsymbol{\omega}_L + \mathbf{g}_L = G\mathbf{f} + G_H\mathbf{f}_H, \tag{2a}$$
$$B_R\ddot{\boldsymbol{\gamma}} + C_R\dot{\boldsymbol{\gamma}} + \mathbf{g}_R = \boldsymbol{\tau} - J_R^\top\mathbf{f}, \tag{2b}$$

with $M \in \mathbb{R}^{6\times6}$ the inertial matrix of (L), with $I_L \in \mathbb{R}^{3\times3}$ its rotation inertia in $\{\mathcal{B}\}$, and $\mathbf{g}_L \in \mathbb{R}^6$ the gravitational terms for (L); $B_R, C_R \in \mathbb{R}^{N\times N}$ the inertial and Coriolis matrices for (R), and $\mathbf{g}_R$ the gravitational terms for (R). In turn, the control input of the system (2) are the (R) joint torques $\boldsymbol{\tau} \in \mathbb{R}^N$, which is applied on to (L) via the generalised contact forces $\mathbf{f} \in \mathbb{R}^{6n}$ in (2a) (see Fig. 3), where $G \in \mathbb{R}^{6\times6n}$ denotes the (R) grasp matrix, given for $\mathbf{f}$ in $\{\mathcal{I}\}$ [27] by

$$G := \left(\begin{array}{cc|c|cc} I_3 & 0_3 & \cdots & I_3 & 0_3 \\ \mathbf{r}_1^\times & I_3 & & \mathbf{r}_n^\times & I_3 \end{array}\right), \quad \mathbf{r}_i := \mathbf{s} - \mathbf{p}_i.$$

On the other hand, the well-known flexible joint RM model in [28] is employed to represent the intrinsic complexity of (H) (see Assumption A4 below), namely

$$B_H^l\ddot{\boldsymbol{\eta}} + C_H\dot{\boldsymbol{\eta}} + K\boldsymbol{\delta} + \mathbf{g}_H = -J_H^\top\mathbf{f}_H, \tag{3a}$$
$$B_H^m\ddot{\boldsymbol{\mu}} - K\boldsymbol{\delta} = \boldsymbol{\tau}_H, \tag{3b}$$

where the friction terms are assumed to be negligible [28]; $B_H^l, B_H^m, C_H^l, C_H^m \in \mathbb{R}^{7\times7}$ are the inertial and Coriolis matrices for (H) –with super-index l and m referring to the link and motor DoF–, and $\mathbf{g}_H$ denotes the gravitational terms for (H); K the *unknown* stiffness of the flexible DoF of (H); and $\mathbf{f}_H$ the forces and torques exerted by (H) to (L) through the grasp matrix $G_H \in \mathbb{R}^{6\times6}$, given for $\mathbf{f}_H$ in $\{\mathcal{I}\}$ [27] by

$$G_H := \begin{pmatrix} I_3 & 0_3 \\ \mathbf{r}_H^\times & I_3 \end{pmatrix}, \quad \mathbf{r}_H := \mathbf{s} - \mathbf{q}.$$

C. Assumptions

Throughout the manuscript, a series of common assumptions are used to formulate the proposed controller, namely

- A1. The references $\mathbf{x}_{L_r}$ and $\mathbf{p}_r$ are feasible.
- A2. The Jacobians J_R and J_H are full-ranked.
- A3. T_L is full-ranked, i.e. $\theta \neq \pm\pi/2$.
- A4. Similarly to variable impedance approaches like [5], [11], [29] –but in the joint-space instead of the operational space–, (H) is assumed to be equivalent to a RM with flexible-actuated compound joints (3), in which:
  - A4.1. The joint velocities of (H) are small and, thus, the equilibrium configuration coincides with the initial configuration, i.e. $\boldsymbol{\mu}(0) = \boldsymbol{\eta}(0)$, and does not move beyond a small area, i.e. $\boldsymbol{\mu}(t) \approx \boldsymbol{\mu}(0),\ \forall t \geq 0$.
  - A4.2. The (H) actuation $\boldsymbol{\tau}_H$ in (3b) cancels the inertial, gravitational and Coriolis terms, i.e. $\boldsymbol{\tau}_H = -K\boldsymbol{\delta} - B_H^m\ddot{\boldsymbol{\delta}} - B_H^m(B_H^l)^{-1}(C_H\dot{\boldsymbol{\eta}} + \mathbf{g}_H)$, while the external forces are compensated by the flexible modes, i.e. $K\boldsymbol{\delta} = -J_H^\top\mathbf{f}_H$.

D. Simplified (H) model

While (R) is the actuated agent used to control (L), (H) can be seen as an *ambiguous* external disturbance to the system. Accordingly, we propose estimating the forces and torques applied by (H) from the deflection of their flexible modes and coping with the induced uncertainty via an adaptive controller on K. For this purpose, a simplified –and inherently pseudo-static– model of the human arm response is obtained under the assumptions in A4:

$$K\boldsymbol{\delta} = \mathbf{d}_H - J_H^\top\mathbf{f}_H, \tag{4}$$

where $\mathbf{d}_H \in \mathbb{R}^7$ is an *unknown* slow time-varying disturbance modelling the small deviations in (3) from assumption A4.2, which are also coped via an adaptive update law. It is worth noting that as (H) has 7 DoF, (4) lacks –in general– a solution for $\mathbf{f}_H$. Nevertheless, from a physical point of view, (4) describes how the flexibility-related generalised forces are distributed throughout these flexible joints. Accordingly, a real distribution of joint-space torques corresponds to a real value of $\mathbf{f}_H$ and, therefore, the lack of a solution is produced by disturbances. Consequently, the least-squares solution given by

$$\hat{\mathbf{f}}_H = (J_H^\top)^\dagger\left[\hat{\mathbf{d}}_H - \hat{K}\boldsymbol{\delta}\right] \tag{5}$$

is considered a suitable estimate to these generalised forces for three reasons: i) due to its formulation, it partially filters the aforementioned noise, ii) it is linear with respect to $\hat{K}$ and $\hat{\mathbf{d}}_H$, and thus suitable for an adaptive approach to cope with the (H) uncertainties, and iii) apart from this update law, the estimation only requires to measure the joint-space configuration of (H) to be implemented.

Remark 1. *It is of interest to compare this estimate with [30] and [23]. In these works, the forces applied at the EE were estimated from the measured joint torques [30] or from these and the angular positions and speeds [23], with the (pseudo)inversion of the full-ranked Jacobian map. In*

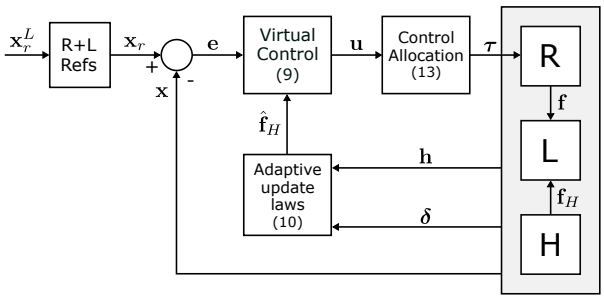

Fig. 3. Control scheme of the proposed strategy (with equation numbers), including the virtual controller and the control allocation.

contrast, we propose applying the same pseudo-inversion to an adaptive estimation of the joint-space torques remaining after assumption A4.2, i.e. $\hat{\mathbf{d}}_H - \hat{K}\boldsymbol{\delta}$.

III. Control strategy

While other controllers tend to only track the (L) pose $\mathbf{x}_L$ [6], [13] or the (R) EE positions $\mathbf{p}$ [11], [14], an approach tracking both at the same time –i.e. $\mathbf{x} := [\mathbf{x}_L^\top, \mathbf{p}^\top]^\top \in \mathbb{R}^S$, $S := 6 + 3n$– is here proposed (see Fig. 3). This concept implies that, while using (R) to indirectly shape the dynamics of (L) to reach a desired configuration, the manipulators converge at the same time to positions consistent with such configuration. As a result of this consistency, disturbances and uncertainties in the dynamic models of (L) or (R) are mitigated. This mitigation, nonetheless, can still be improved. For this purpose, an adaptive update law to cope with human interaction uncertainties is additionally proposed.

Considering this, and that the dynamic equations in (2) are written in a mixed inertial and body frame form for (L) and in the joint-space for (R), let us define a velocity fitting with these spaces as $\mathbf{v}^\top := [\mathbf{v}_L^\top, \dot{\boldsymbol{\gamma}}^\top]$, with $\dot{\mathbf{x}} = W\mathbf{v}$ and

$$W = \begin{pmatrix} \mathbb{T}_L^{-1} & 0 \\ 0 & J_R^p \end{pmatrix}.$$

Then, under the assumptions A2 and A3, the kinematics (1a)-(1b) and dynamics (2a)-(2b) on the combined (R)+(L) system can be rewritten in error terms (see Appendix A-A) as

$$\dot{\mathbf{e}}_I = \mathbf{e}_P, \tag{6a}$$

$$\dot{\mathbf{e}}_P = \mathbf{e}_D, \tag{6b}$$

$$\dot{\mathbf{e}}_D = \ddot{\mathbf{x}}_r + \dot{W}W^+(\mathbf{e}_D - \dot{\mathbf{x}}_r) - WB^{-1}(\mathbf{u} + \mathbf{u}_H - \mathbf{b}), \tag{6c}$$

where $\mathbf{e}_P := \mathbf{x}_r - \mathbf{x}$ is the tracking error and $\mathbf{e}_I$ its implicit integral counterpart;

$$B = \begin{pmatrix} M & 0 \\ 0 & B_R \end{pmatrix}$$

the inertia matrix of the whole system, and

$$\mathbf{u} := \begin{bmatrix} \mathbf{0}_6 \\ \boldsymbol{\tau} \end{bmatrix} + \begin{pmatrix} G \\ -J_R^\top \end{pmatrix} \mathbf{f}, \tag{7}$$

$$\mathbf{u}_H := \begin{bmatrix} G_H \mathbf{f}_H \\ \mathbf{0}_N \end{bmatrix}, \tag{8}$$

the virtual control input and its associated representation of the effects of (H) on the (R)+(L) system via the grasping of (L); and $\mathbf{b}^\top = [(\boldsymbol{\omega}_L^\times I_L \boldsymbol{\omega}_L)^\top + \mathbf{g}_L^\top, (C_R\dot{\boldsymbol{\gamma}})^\top + \mathbf{g}_R^\top]$.

Remark 2. *It is worth noting that the virtual control input variable* $\mathbf{u}$ *is an intermediate state derived from the real control input* $\boldsymbol{\tau}$ *whose internal coupling –in this case, through* $\mathbf{f}$ *in (7)– is not explicitly considered. This virtual tool is used to simplify the design of the controller, while* $\boldsymbol{\tau}$ *is later obtained in (13) from a particular control allocation.*

Among the different approaches fitting the virtual problem in (6), an adaptive integral backstepping approach is chosen: i) adaptive to cope with the (H) uncertainties, and ii) integral to handle zero steady-state error. This controller is given by

$$\mathbf{u} = BW^+ \left(\Gamma \mathbf{e} + \ddot{\mathbf{x}}_r - \dot{W}W^+ \dot{\mathbf{x}}_r \right) + \mathbf{b} - \hat{\mathbf{u}}_H, \tag{9}$$

with $\mathbf{e} := [\mathbf{e}_I^\top, \mathbf{e}_P^\top, \mathbf{e}_D^\top]^\top$, $\hat{\mathbf{u}}_H^\top := [(G_H\hat{\mathbf{f}}_H)^\top, \mathbf{0}_N^\top]$ and $\Gamma := (\Gamma_I, \Gamma_P, \Gamma_D + \dot{W}W^+)$,

$$\begin{aligned} \Gamma_I &:= \Gamma_1 + \Gamma_3\Gamma_2\Gamma_1 + \Gamma_3, \\ \Gamma_P &:= \Gamma_2\Gamma_1 + \Gamma_3\Gamma_1 + \Gamma_3\Gamma_2 + 2I_S, \\ \Gamma_D &:= \Gamma_1 + \Gamma_2 + \Gamma_3, \end{aligned}$$

where $\Gamma_1, \Gamma_2, \Gamma_3 \in \mathbb{R}^{S\times S}$ are positive definite gain matrices; along with the adaptive update laws for the estimate of (8) –with $\hat{\mathbf{f}}_H$ defined in (5)– given by

$$\dot{\hat{\mathbf{d}}}_H = -\Gamma_d \mathbf{h}, \tag{10a}$$

$$\dot{\hat{K}} = \Gamma_K \boldsymbol{\delta} \mathbf{h}^\top, \tag{10b}$$

with $\Gamma_d, \Gamma_K \in \mathbb{R}^{7\times7}$ positive definite, $\mathbf{h} := \Lambda_h \Gamma_h \mathbf{e}$ a vector encapsulating the connection between (L) and the human-related disturbances, $\Lambda_h := (J_H^\dagger G_H^T M^{-1} \mathbb{T}_L^{-T}, 0_{7\times6})$, and $\Gamma_h := (\Gamma_2\Gamma_1 + I_S, \Gamma_2 + \Gamma_1, I_S)$.

Proposition 1. *Consider the system (6) and the estimation of* $\mathbf{f}_H$ *in (5) under the assumptions A1-A4 in Subsection II-C. Then, under the control law (9) and its associated adaptive update laws (10), the closed-loop system is asymptotically stabilised to zero, i.e.* $\mathbf{e} \to \mathbf{0}$ *as* $t \to \infty$.

Proof. Let us define $V_1 := |\mathbf{e}_I|^2/2 \geq 0$, whose time derivative reads $\dot{V}_1 = \mathbf{e}_I^\top \mathbf{e}_P = -\mathbf{e}_I^\top \Gamma_1 \mathbf{e}_I - \mathbf{z}_1^\top \mathbf{e}_I$, with $\mathbf{z}_1 := -\Gamma_1 \mathbf{e}_I - \mathbf{e}_P$ being the error of the first step. To cope with it, we define $V_2 := V_1 + |\mathbf{z}_1|^2/2 \geq 0$, whose derivative is $\dot{V}_2 = -\mathbf{e}_I^\top \Gamma_1 \mathbf{e}_I - \mathbf{z}_1^\top (\mathbf{e}_I + \Gamma_1 \mathbf{e}_P + \mathbf{e}_D) = -\mathbf{e}_I^\top \Gamma_1 \mathbf{e}_I - \mathbf{z}_1^\top \Gamma_2 \mathbf{z}_1 - \mathbf{z}_2^\top \mathbf{z}_1$, with $\mathbf{z}_2 := -\Gamma_2 \mathbf{z}_1 + \mathbf{e}_I + \Gamma_1 \mathbf{e}_P + \mathbf{e}_D$ the error of this second step. To cope with it, in turn, $V_3 := V_2 + |\mathbf{z}_2|^2/2 \geq 0$ is used. The derivative of this function (see Appendix A-B) therefore reads

$$\begin{aligned} \dot{V}_3 &= -\mathbf{e}_I^\top \Gamma_1 \mathbf{e}_I - \mathbf{z}_1^\top \Gamma_2 \mathbf{z}_1 \\ &\quad + \mathbf{z}_2^\top \Big[\Gamma_1 \mathbf{e}_I + (\Gamma_2\Gamma_1 + 2I_S)\, \mathbf{e}_P + (\Gamma_2 + \Gamma_1)\, \mathbf{e}_D \\ &\quad + \ddot{\mathbf{x}}_r + \dot{W}W^+(\mathbf{e}_D - \dot{\mathbf{x}}_r) - WB^{-1}(\mathbf{u} + \mathbf{u}_H - \mathbf{b}) \Big], \\ &= -\mathbf{e}_I^\top \Gamma_1 \mathbf{e}_I - \mathbf{z}_1^\top \Gamma_2 \mathbf{z}_1 - \mathbf{z}_2^\top \Gamma_3 \mathbf{z}_2 - \mathbf{h}^\top \left(\tilde{\mathbf{d}}_H - \tilde{K}\boldsymbol{\delta} \right). \end{aligned}$$

As the only potentially nonnegative terms in $\dot{V}_3$ are produced by the disturbances associated with (H), i.e. $J_H^\top \tilde{\mathbf{f}}_H = \tilde{\mathbf{d}}_H - \tilde{K}\boldsymbol{\delta}$, the final Lyapunov function is chosen, namely

$$V_A := V_3 + \frac{1}{2}\tilde{\mathbf{d}}_H^\top \Gamma_d^{-1} \tilde{\mathbf{d}}_H + \frac{1}{2}\mathrm{tr}\left(\tilde{K}^\top \Gamma_K^{-1} \tilde{K} \right).$$

The derivative of this function is given by

$$\begin{aligned}\dot{V}_A =& -\mathbf{e}_I^\top \Gamma_1 \mathbf{e}_I - \mathbf{z}_1^\top \Gamma_2 \mathbf{z}_1 - \mathbf{z}_2^\top \Gamma_3 \mathbf{z}_2 \\ & - \mathbf{h}^\top \left(\tilde{\mathbf{d}}_H - \tilde{K}\boldsymbol{\delta}\right) + \tilde{\mathbf{d}}_H^\top \Gamma_d^{-1} \dot{\tilde{\mathbf{d}}}_H + \mathrm{tr}\left(\tilde{K}^\top \Gamma_K^{-1} \dot{\tilde{K}}\right) \\ =& -\mathbf{e}_I^\top \Gamma_1 \mathbf{e}_I - \mathbf{z}_1^\top \Gamma_2 \mathbf{z}_1 - \mathbf{z}_2^\top \Gamma_3 \mathbf{z}_2 \\ & + \tilde{\mathbf{d}}_H^\top \left(\Gamma_d^{-1} \dot{\tilde{\mathbf{d}}}_H - \mathbf{h}\right) + \mathrm{tr}\left[\tilde{K}^\top \left(\Gamma_K^{-1} \dot{\tilde{K}} + \boldsymbol{\delta}\mathbf{h}^\top\right)\right].\end{aligned}$$

Finally, upon plugging (10) into this derivative, we obtain

$$\dot{V}_A = -\mathbf{e}_I^\top \Gamma_1 \mathbf{e}_I - \mathbf{z}_1^\top \Gamma_2 \mathbf{z}_1 - \mathbf{z}_2^\top \Gamma_3 \mathbf{z}_2 \leq 0. \tag{11}$$

Therefore, since both auxiliary error variables are defined s.t. $\mathbf{z}_1 = \mathbf{0} \equiv \mathbf{e}_I, \mathbf{e}_P = \mathbf{0}$ and $\mathbf{z}_2 = \mathbf{0} \equiv \mathbf{e}_I, \mathbf{e}_P, \mathbf{e}_D = \mathbf{0}$, the Lyapunov function derivative $\dot{V}_A = 0 \equiv \mathbf{e} = \mathbf{0}$, thus concluding the proof. □

The (R) forces on the load can be then determined by pre-multiplying (7) by $(I_6, 0_N)$, namely

$$\mathbf{f} = G^+ \begin{pmatrix} I_6 & 0_N \end{pmatrix} \mathbf{u}, \tag{12}$$

where the right-hand pseudoinverse of the *full-ranked* grasp matrix G produces the minimal actuation needed to meet the virtual requirements. It is worth noting that adding terms in the nullspace of G would have no interest for fixed grasping as these would only result in internal forces in (L) [27]. Pre-multiplying (7) by $(0_6, I_N)$ and plugging (12), the control input that replicates the effects of (7) on the system reads

$$\boldsymbol{\tau} = \begin{pmatrix} J_R^\top G^+ & I_N \end{pmatrix} \mathbf{u}. \tag{13}$$

Combining the virtual controller (9) and the control allocation (13), the final real control law for the system is

$$\boldsymbol{\tau} = \Lambda \left(\Gamma \mathbf{e} + \ddot{\mathbf{x}}_r - \dot{W} W^+ \dot{\mathbf{x}}_r\right) + J_R^\top G^+ (\mathbf{b}_L - G_H \hat{\mathbf{f}}_H) + \mathbf{b}_R, \tag{14}$$

with

$$\Lambda := \begin{pmatrix} J_R^\top G^+ M \mathbb{T}_L & B_R (J_R^p)^+ \end{pmatrix}.$$

IV. Experimental validation

To validate the proposed control strategy, we test the robustness of the solution against implementation disturbances and the *ambiguous* human interaction (Fig. 1). The validation experiments are carried out with and without[2] updating the adaptive law in (10) in three scenarios: i) (H) trying to assist (R), ii) (H) having no interaction with (R), and iii) (H) actively disturbing (R). While the second scenario is chosen as a control case showing the basic capabilities of the strategy, i) is designed to evaluate if the solution fits a nominal HRC task and analyse the impact human help; and iii) is specifically aimed at validating the disturbance rejection capabilities obtained with both contribution C1 and C2. Furthermore, these cases are studied with and without updating the adaptive laws to identify which advances correspond mainly to C2 (without) and which to C1 (with).

In the three scenarios the same (L) references are given for consistency. These are chosen to pose a challenge to the manipulation system even without disturbances: relatively fast displacements for manipulation tasks requiring high accuracy ($\sim$0.1 m/s) going through varied regions of the manipulability ellipsoid for the position tracking, and slower but wide attitude references demanding significant reconfigurations of the manipulators themselves. Furthermore, the experiments including interactions are performed in a strict sequence so that the operator forces and motion are as consistent as possible, i.e. following a choreography for the experiment without adaptive laws and, immediately afterwards, repeating it for the one with the adaptive module. Although this approach has limitations, the operator achieved an acceptable degree of repeatability, as evinced in Fig. 4 by the repetition of certain error peaks at similar times.

TABLE I
Control gains

Agent	Component	Γ_1	Γ_2	Γ_3
(L)	All positions	0.5	30.0	6.0
	Roll and pitch	1.5	120.0	6.0
	Yaw	0.6	160.0	0.8
(R)	Horizontal position	0.4	9.0	4.0
	Vertical position	0.6	18.0	4.0

Agent	Component	Γ_K	Γ_d	σ
(H)	All	0.15	0.15	200

The hardware consists of 2 6-DoF HEBI Robotics A-2085-06 [31] RMs whose bases are the origin of $\{\mathcal{I}\}$, for $(\mathrm{R})_1$, and displaced $0.987\mathrm{m}$ in direction Y, for $(\mathrm{R})_2$ (see Fig. 2); a load of mass $2.117\mathrm{kg}$ (above the sum of the maximum payloads of both RMs) and moments of inertia in $\{\mathcal{B}\}$ $I_{L_x} = 0.0297\mathrm{kg\,m^2}$, $I_{L_y} = 0.0316\mathrm{kg\,m^2}$ and $I_{L_z} = 0.0440\mathrm{kg\,m^2}$, where the grasping points in $\{\mathcal{B}\}$ are $\mathbf{r}_1 = [0, -0.145, 0]^\top \mathrm{m}$, $\mathbf{r}_2 = [0, 0.145, 0]^\top \mathrm{m}$ and $\mathbf{r}_H = [0.153, 0.145, -0.085]^\top \mathrm{m}$; and a computer equipped with a Intel Core i7-1085-H CPU at 2.70 GHz and 32 GB of RAM (DDR4). The feedback is obtained both from the sensors mounted on (R), and from a Qualisys Motion Capture System [32] with 12 Ocus-400 cameras for (H). Regarding software, the controller runs in real-time at $100\mathrm{Hz}$ using the Robotic Systems Toolbox [33] in Simulink, with the control gains in Table I. This includes a σ-modification of the adaptive update laws to cope with noise-induced drift [34]. For the connection between the computer and (R), the HEBI MATLAB API [35] is employed. In turn, the Simulink ROS Toolbox is used to subscribe to the motion capture data for (L) and (H).

Moving to the validation, we here analyse the experimental results.[3] As shown in Fig. 4, the controller is capable of tracking all the references without the adaptive update law when there is no interaction. It is specially significant that the response of base strategy in attitude is acceptably smooth and shows no noticeable steady state error. However, the lack of compensation without updating the parameters –and specially under disturbances– clearly results in a poorer tracking performance. Not only can be this seen in the attitude

[2]Setting an empirical trade-off value for the adaptive parameters.

[3]Video available at https://youtu.be/syHMfUN0SyE.

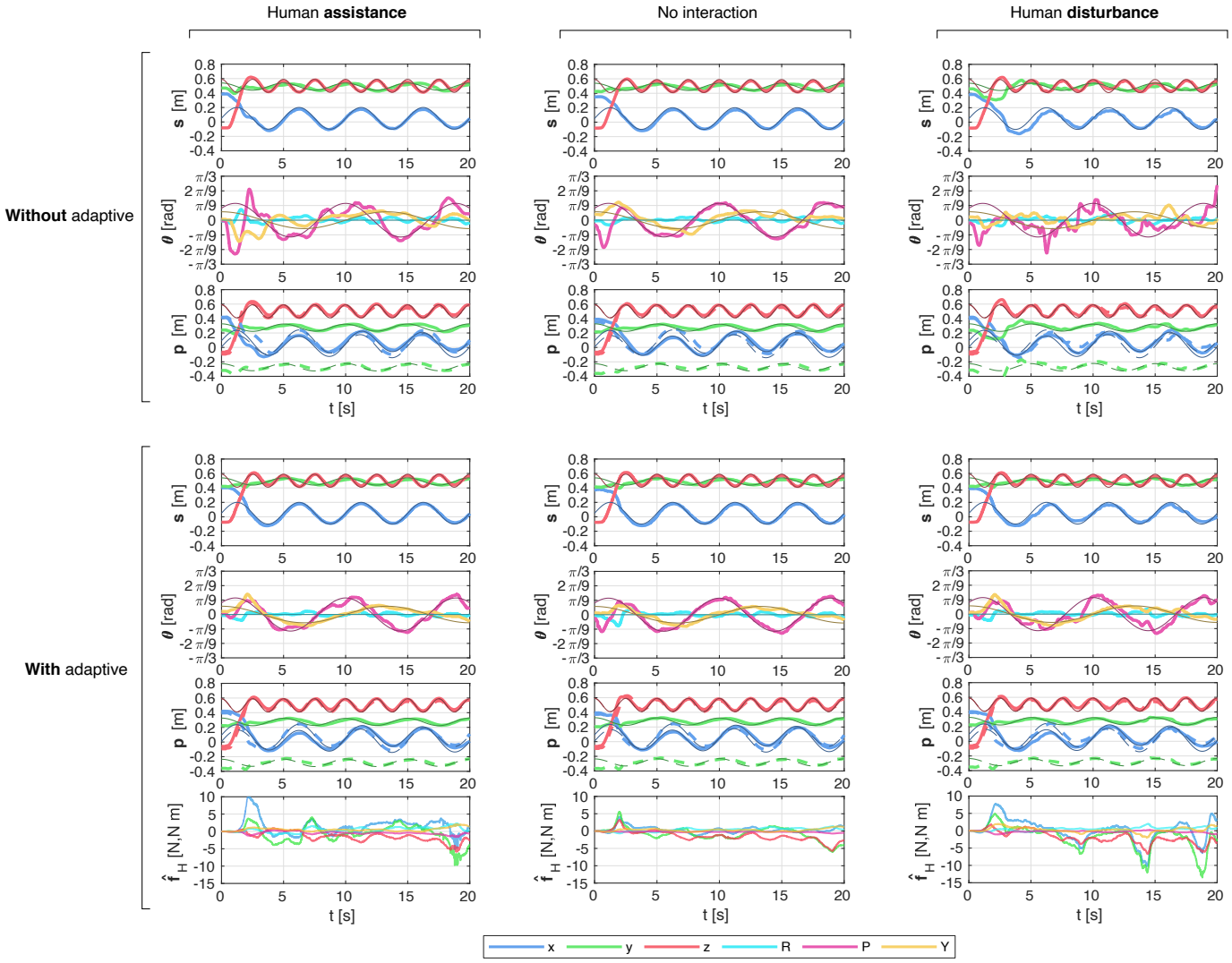

Fig. 4. Experimental results with and without the adaptive update law (10) under three scenarios: human assistance, no interaction, and human disturbance. The components of each variable are displayed using the colour scheme in the bottom legend (where R, P, Y stand for roll, pitch and yaw) –with their associated references being thinner and darker–, and $\mathbf{p}_1$ and $\mathbf{p}_2$ are shown using solid and dashed lines, respectively.

tracking response, which is considerable less robust and shows substantial oscillations, but also in the deterioration of the transient response in positions and the –small but significant– presence of steady-state error. This situation, nonetheless, does not reach unstable behaviours, and the base of the strategy (i.e. the *simultaneous* tracking of the (L) and (R) references) is shown to provide a robust –but improvable– foundation upon which the adaptive update law is added to cope with this downgrade during interaction.

In contrast, the complete strategy maintains the nominal tracking performance during the HRI thanks to the compensation coming from $\hat{\mathbf{f}}_H$ (last row, Fig. 4). For instance, while without it the disturbances produced noticeable oscillations in the (L) attitude, these are here comparable to the human-assisted adaptive case, significantly smoother than the scenario without adaptive updates, and just slightly wider in amplitude than the control case. In turn, a comparison between both cases in the x component of the (L) position tracking shows that the controller with the adaptive law is smoother and faster during the initial transient than the base one, and it does not display significant steady-state error.

Moving to the $\hat{\mathbf{f}}_H$ terms themselves, these evolve under excitation to make the response smoother and, under significant disturbances, (such as at 14 s or 17 s for the human disturbance case) to mitigate these external actions. Moreover, a pattern can be detected if we compare the response with the adaptive laws for both interaction cases: the generalised force profiles are similar for both, with just a more aggressive response of the update laws under disturbances, as expected. It is also worth noting that –apart from a peak in x during the initial transient– these profiles show forces whose main components are in y and z, corresponding to the main directions in which the forces in the interaction cases were applied. It is also worth highlighting that the complete strategy also improves the already solid response of the base controller without interactions (central column in Fig. 4), specially for smoothening the attitude response.

TABLE II
STATISTICAL ANALYSIS, RMSE [m, rad]

		$\mathbf{x}_L$						$\mathbf{p}_1$			$\mathbf{p}_2$		
		x	y	z	ϕ	θ	ψ	x	y	z	x	y	z
Transient ($t < 5$s)	Without adaptive	0.118	0.058	0.272	0.066	0.454	0.196	0.107	0.055	0.259	0.160	0.064	0.276
	With adaptive	0.124	0.050	0.278	0.079	0.308	0.156	0.114	0.046	0.264	0.140	0.053	0.285
	Variation (%)	*4.76*	*-13.01*	*2.44*	*19.82*	*-32.10*	*-20.09*	*6.73*	*-17.53*	*2.04*	*-12.02*	*-17.98*	*3.25*
Steady-state ($t \geq 5$s)	Without adaptive	0.025	0.023	0.017	0.049	0.158	0.123	0.041	0.022	0.018	0.041	0.022	0.023
	With adaptive	0.027	0.019	0.016	0.041	0.108	0.059	0.032	0.019	0.017	0.032	0.022	0.020
	Variation (%)	*9.37*	*-17.23*	*-6.65*	*-15.75*	*-31.84*	*-51.58*	*-21.86*	*-11.54*	*-1.65*	*-22.79*	*-0.53*	*-14.33*

Finally, we include a broader statistical analysis to quantify the solidity of the base strategy and the improvements due to the adaptive modification. For that purpose, we analyse the transient and steady-state regimes[4] of the strategy with and without the adaptive update law (Table IV). These two cases are evaluated in terms of root-mean-square error (RMSE) for 16 separate experiments which prioritise the disturbance rejection: 4 human-assisted, 4 without interaction, and 8 human-disturbed; half of the experiments per scenario with and the other half without the adaptive update law.

This analysis shows that the performance of both the base and the complete solution are similar during transients, with comparable position errors and a marginally superior attitude response for the complete strategy. In both cases, nonetheless, the transient performance is sufficient for the fast and nontrivial tracking scenario proposed. For instance, the (L) position norm RMSE in both is $\sim$30 cm for a reference change of $\sim$85 cm, which is comparable to a first-order response with a time constant (63%) of 1.2 s.

In contrast, the advances in the steady-state regime due to the adaptive estimation of the human-induced wrench are substantial. The complete strategy clearly outperforms the base solution in all variables included in the task-space, except for the x position of the load –which grows marginally–, and z position of $(R)_1$ and y position of $(R)_2$ –whose decrease is insignificant–. This improvement is especially important in the (L) attitude, where the yaw RMSE is halved and the overall orientation error (in norm) is reduced by a 37% –from 0.21 rad (12°) to 0.13 rad (7°)–, as already detected in the analysis of the results in Fig. 4.

V. CONCLUSION

In this letter, we developed an adaptive controller for the shared manipulation of loads between human and robotic agents. The proposed solution simultaneously tracks the consistent references for both the load and the robot end-effectors under the *ambiguous* collaboration of a human agent, whose influence on the load and robot dynamics is compensated with an adaptive update law. The results include a theoretical stability analysis and a detailed experimental validation. Future work includes the redesign of the proposed controller to exploit the redundancy of (R) to avoid singular configurations, allowing us to relax assumption A2.

[4]The transition between both has been empirically set to $t = 5$s.

ACKNOWLEDGMENT

The authors thank Gil Silvestre Serrano and Robin Baran for their contribution to the experimental validation.

REFERENCES

[1] A. Billard and D. Kragic, "Trends and challenges in robot manipulation," *Science*, vol. 364, no. 6446, 2019.

[2] A. Ajoudani, A. M. Zanchettin, S. Ivaldi, A. Albu-Schäffer, K. Kosuge, and O. Khatib, "Progress and prospects of the human–robot collaboration," *Autonomous Robots*, vol. 42, no. 5, pp. 957–975, 2018.

[3] J. P. Vasconez, G. A. Kantor, and F. A. Auat Cheein, "Human–robot interaction in agriculture: A survey and current challenges," *Biosystems Engineering*, vol. 179, pp. 35–48, 2019.

[4] W. S. Cortez, C. Verginis, and D. V. Dimarogonas, "Safe, Passive Control for Mechanical Systems with Application to Physical Human-Robot Interactions," in *2021 IEEE International Conference on Robotics and Automation (ICRA)*. IEEE, 2021.

[5] T. Tsumugiwa, R. Yokogawa, and K. Hara, "Variable impedance control based on estimation of human arm stiffness for human-robot cooperative calligraphic task," in *2002 IEEE International Conference on Robotics and Automation (ICRA)*, vol. 1, 2002, pp. 644–650 vol.1.

[6] M. Mujica, M. Benoussaad, and J.-Y. Fourquet, "Evaluation of human-robot object co-manipulation under robot impedance control," in *2020 IEEE International Conference on Robotics and Automation (ICRA)*, 2020, pp. 9143–9149.

[7] M. Sharifi, S. Behzadipour, and G. Vossoughi, "Nonlinear model reference adaptive impedance control for human–robot interactions," *Control Engineering Practice*, vol. 32, pp. 9–27, 2014.

[8] H.-C. Lin, J. Smith, K. K. Babarahmati, N. Dehio, and M. Mistry, "A Projected Inverse Dynamics Approach for Multi-Arm Cartesian Impedance Control," in *2018 IEEE International Conference on Robotics and Automation (ICRA)*, 2018, pp. 5421–5428.

[9] Agravante, Don Joven and Cherubini, Andrea and Bussy, Antoine and Gergondet, Pierre and Kheddar, Abderrahmane, "Collaborative human-humanoid carrying using vision and haptic sensing," in *2014 IEEE International Conference on Robotics and Automation (ICRA)*, 2014, pp. 607–612.

[10] M. Lawitzky, A. Mörtl, and S. Hirche, "Load sharing in human-robot cooperative manipulation," in *19th International Symposium in Robot and Human Interactive Communication*, 2010, pp. 185–191.

[11] C. N. Mavridis, K. Alevizos, C. P. Bechlioulis, and K. J. Kyriakopoulos, "Human-robot collaboration based on robust motion intention estimation with prescribed performance," in *2018 European Control Conference (ECC)*, 2018, pp. 249–254.

[12] M. Lippi and A. Marino, "Human multi-robot physical interaction: a distributed framework," *Journal of Intelligent & Robotic Systems*, vol. 101, no. 2, pp. 1–20, 2021.

[13] B. Nemec, N. Likar, A. Gams, and A. Ude, "Bimanual human robot cooperation with adaptive stiffness control," in *2016 IEEE-RAS International Conference on Humanoid Robots (Humanoids)*, 2016, pp. 607–613.

[14] N. Dehio, J. Smith, D. L. Wigand, G. Xin, H.-C. Lin, J. J. Steil, and M. Mistry, "Modeling and control of multi-arm and multi-leg robots: Compensating for object dynamics during grasping," in *2018 IEEE International Conference on Robotics and Automation (ICRA)*. IEEE, 2018, pp. 294–301.

[15] L. Gracia, J. E. Solanes, P. Muñoz-Benavent, A. Esparza, J. Valls Miro, and J. Tornero, "Cooperative transport tasks with robots using adaptive non-conventional sliding mode control," *Control Engineering Practice*, vol. 78, pp. 35–55, 2018.

[16] M. Lippi, G. Gillini, A. Marino, and F. Arrichiello, "A data-driven approach for contact detection, classification and reaction in physical human-robot collaboration," in *2021 IEEE International Conference on Robotics and Automation (ICRA)*. IEEE, 2021.

[17] R. Hayne, R. Luo, and D. Berenson, "Considering avoidance and consistency in motion planning for human-robot manipulation in a shared workspace," in *2016 IEEE International Conference on Robotics and Automation (ICRA)*, 2016, pp. 3948–3954.

[18] KTH Royal Institute of Technology, "Smart Mobility Lab," https://www.kth.se/is/dcs/research/control-of-transport/smart-mobility-lab/smart-mobility-lab-1.441539, online; accessed 4 February 2022.

[19] Culbertson, Preston and Slotine, Jean-Jacques and Schwager, Mac, "Decentralized Adaptive Control for Collaborative Manipulation of Rigid Bodies," *IEEE Transactions on Robotics*, vol. 37, no. 6, pp. 1906–1920, 2021.

[20] Yan, Lei and Stouraitis, Theodoros and Vijayakumar, Sethu, "Decentralized Ability-Aware Adaptive Control for Multi-Robot Collaborative Manipulation," *IEEE Robotics and Automation Letters*, vol. 6, no. 2, pp. 2311–2318, 2021.

[21] C. R. de Cos, J. Á. Acosta, and A. Ollero, "Adaptive Integral Force Control for Lightweight Flexible Manipulators," *Preprint*, 2021.

[22] CANOPIES project, "A Collaborative Paradigm for Human Workers and Multi-Robot Teams in Precision Agriculture Systems," in *https://www.project-canopies.eu/*. European Commission under the H2020 Framework Programme. [Online]. Available: https://www.project-canopies.eu/

[23] F. Ficuciello, L. Villani, and B. Siciliano, "Variable impedance control of redundant manipulators for intuitive human–robot physical interaction," *IEEE Transactions on Robotics*, vol. 31, no. 4, pp. 850–863, 2015.

[24] C. R. de Cos, J. A. Acosta, and A. Ollero, "Adaptive integral inverse kinematics control for lightweight compliant manipulators," *IEEE Robotics and Automation Letters*, vol. 5, no. 2, pp. 282–289, April 2020.

[25] B. Siciliano, L. Sciavicco, L. Villani, and G. Oriolo, *Robotics. Modelling, planning and control*. Springer-Verlag (UK), 2009.

[26] G. Averta, C. Della Santina, E. Battaglia, F. Felici, M. Bianchi, and A. Bicchi, "Unvealing the principal modes of human upper limb movements through functional analysis," *Frontiers in Robotics and AI*, vol. 4, p. 37, 2017. [Online]. Available: https://www.frontiersin.org/article/10.3389/frobt.2017.00037

[27] B. Siciliano and O. Khatib, *Springer handbook of robotics*. springer, 2016.

[28] A. De Luca, A. Albu-Schaffer, S. Haddadin, and G. Hirzinger, "Collision detection and safe reaction with the dlr-iii lightweight manipulator arm," in *2006 IEEE/RSJ International Conference on Intelligent Robots and Systems*. IEEE, 2006, pp. 1623–1630.

[29] M. Dyck and M. Tavakoli, "Measuring the dynamic impedance of the human arm without a force sensor," in *2013 IEEE 13th International Conference on Rehabilitation Robotics (ICORR)*, 2013, pp. 1–8.

[30] D. Kruse, R. J. Radke, and J. T. Wen, "Collaborative human-robot manipulation of highly deformable materials," in *2015 IEEE International Conference on Robotics and Automation (ICRA)*, 2015, pp. 3782–3787.

[31] HEBI Robotics, "A-2085-06 Robotic Arm," https://www.hebirobotics.com/a-2085-06, online; accessed 12 September 2021.

[32] Qualisys AB, "Qualisys Motion Capture System," https://www.qualisys.com/, online; accessed 12 September 2021.

[33] MathWorks, "Robotics System Toolbox," https://uk.mathworks.com/products/robotics.html, online; accessed 12 September 2021.

[34] P. Ioannou and J. Sun, *Robust Adaptive Control*, ser. Dover Books on Electrical Engineering Series. Dover Publications, Incorporated, 2012. [Online]. Available: https://books.google.es/books?id=pXWFY_vbg1MC

[35] HEBI Robotics, "HEBI Robotics MATLAB API," https://docs.hebi.us/tools.html#matlab-api, online; accessed 12 September 2021.

APPENDIX A
DETAILED DERIVATIONS

A. (R)+(L) system model in error terms

We focus here on the derivations to obtain (6c), as the other parts of (6) are straightforward applications of the definition of $\mathbf{e}_P$ and $\mathbf{e}_D$. Upon plugging $\dot{\mathbf{x}} = W\mathbf{v}$ into the definition of $\mathbf{e}_D$, we obtain

$$\begin{aligned}\dot{\mathbf{e}}_D &= \ddot{\mathbf{x}}_r - \ddot{\mathbf{x}} = \ddot{\mathbf{x}}_r - \dot{W}\mathbf{v} - W\dot{\mathbf{v}} \\ &= \ddot{\mathbf{x}}_r + \dot{W}W^{+}\left(\mathbf{e}_D - \dot{\mathbf{x}}_r\right) - W\dot{\mathbf{v}},\end{aligned}$$

where W^{+} can be used as per assumptions A2 and A3. Then, we use (2) and the definition of B to obtain $\dot{\mathbf{v}}$, leading to

$$\begin{aligned}\dot{\mathbf{e}}_D = &\ddot{\mathbf{x}}_r + \dot{W}W^{+}\left(\mathbf{e}_D - \dot{\mathbf{x}}_r\right) \\ &- WB^{-1}\begin{bmatrix} G\mathbf{f} + G_H\mathbf{f}_H - \boldsymbol{\omega}_L^{\times} I_L \boldsymbol{\omega}_L - \mathbf{g}_L \\ \boldsymbol{\tau} - J_R^{\top}\mathbf{f} - C_R\dot{\boldsymbol{\gamma}} - \mathbf{g}_R \end{bmatrix} \\ = &\ddot{\mathbf{x}}_r + \dot{W}W^{+}\left(\mathbf{e}_D - \dot{\mathbf{x}}_r\right) - WB^{-1}\left(\mathbf{u} + \mathbf{u}_H - \mathbf{b}\right),\end{aligned}$$

where the definitions of $\mathbf{u}, \mathbf{u}_H$ –(7) and (8), respectively–, and of $\mathbf{b}$ (above Remark 2) are used for the last step.

B. Derivative of V_3

Using the definitions of V_3, $\mathbf{z}_2$, and (6c), we obtain

$$\begin{aligned}\dot{V}_3 = &-\mathbf{e}_I^{\top}\Gamma_1\mathbf{e}_I - \mathbf{z}_1^{\top}\Gamma_2\mathbf{z}_1 - \mathbf{z}_2^{\top}\mathbf{z}_1 - \mathbf{z}_2^{\top}\dot{\mathbf{z}}_2 \\ = &-\mathbf{e}_I^{\top}\Gamma_1\mathbf{e}_I - \mathbf{z}_1^{\top}\Gamma_2\mathbf{z}_1 \\ &+ \mathbf{z}_2^{\top}\Big[\Gamma_1\mathbf{e}_I + \left(\Gamma_2\Gamma_1 + 2I_S\right)\mathbf{e}_P + \left(\Gamma_2 + \Gamma_1\right)\mathbf{e}_D \\ &+ \ddot{\mathbf{x}}_r + \dot{W}W^{+}(\mathbf{e}_D - \dot{\mathbf{x}}_r) - WB^{-1}(\mathbf{u} + \mathbf{u}_H - \mathbf{b})\Big].\end{aligned}$$

Then, introducing the virtual controller in (9) and taking into account that $\mathbf{z}_2 := \Gamma_h\mathbf{e}$, we get

$$\begin{aligned}\dot{V}_3 = &-\mathbf{e}_I^{\top}\Gamma_1\mathbf{e}_I - \mathbf{z}_1^{\top}\Gamma_2\mathbf{z}_1 - \mathbf{z}_2^{\top}WB^{-1}\tilde{\mathbf{u}}_H \\ &- \mathbf{z}_2^{\top}\Gamma_3\left[\left(\Gamma_2\Gamma_1 + I_S\right)\mathbf{e}_I + \left(\Gamma_2 + \Gamma_1\right)\mathbf{e}_P + \mathbf{e}_D\right] \\ = &-\mathbf{e}_I^{\top}\Gamma_1\mathbf{e}_I - \mathbf{z}_1^{\top}\Gamma_2\mathbf{z}_1 - \mathbf{z}_2^{\top}\Gamma_3\mathbf{z}_2 - \mathbf{e}^{\top}\Gamma_h^{\top}WB^{-1}\tilde{\mathbf{u}}_H.\end{aligned}$$

Let us finally analyse the term $\mathbf{e}^{\top}\Gamma_h^{\top}WB^{-1}\tilde{\mathbf{u}}_H$. Employing the definitions of W, B and $\mathbf{u}_H$, the estimation of the (H) generalised forces in (5), and displaying these in a matricial form, this term becomes

$$\begin{aligned}\mathbf{e}^{\top}\Gamma_h^{\top}WB^{-1}\tilde{\mathbf{u}}_H &= \mathbf{e}^{\top}\Gamma_h^{\top}\begin{pmatrix}\mathbb{T}_L^{-1}M^{-1} & 0 \\ 0 & J_R^{p}B_R^{-1}\end{pmatrix}\begin{bmatrix}G_H\tilde{\mathbf{f}}_H \\ \mathbf{0}_N\end{bmatrix} \\ &= \mathbf{e}^{\top}\Gamma_h^{\top}\begin{bmatrix}\mathbb{T}_L^{-1}M^{-1}G_H(J_H^{\top})^{\dagger}\Big(\tilde{\mathbf{d}}_H - \tilde{K}\boldsymbol{\delta}\Big) \\ \mathbf{0}_N\end{bmatrix} \\ &= \underbrace{\mathbf{e}^{\top}\Gamma_h^{\top}\Lambda_h^{\top}}_{\mathbf{h}^{\top}}\Big(\tilde{\mathbf{d}}_H - \tilde{K}\boldsymbol{\delta}\Big).\end{aligned}$$

Accordingly, the derivative of V_3 becomes

$$\dot{V}_3 = -\mathbf{e}_I^{\top}\Gamma_1\mathbf{e}_I - \mathbf{z}_1^{\top}\Gamma_2\mathbf{z}_1 - \mathbf{z}_2^{\top}\Gamma_3\mathbf{z}_2 - \mathbf{h}^{\top}\Big(\tilde{\mathbf{d}}_H - \tilde{K}\boldsymbol{\delta}\Big),$$

as used in the Proof of Proposition 1 to identify the uncertainties to be coped with the adaptive update law in (10).